Controlled Oxidation of Aluminum Nano and Micro Particles: Modeling and Validation

Giuliana Litrico[⋆]*, Laura Leon Perez*[⋆]*, Pierre Proulx*[⋆⋆]*, Jean - Baptiste Gouriet*[⋆] *and Patrick Rambaud*[⋆]
[⋆]*von Karman Institute for Fluid Dynamics*
BELGIUM
[⋆⋆]*University of Sherbrook*
CANADA

Abstract

A theoretical and experimental analysis of the oxidation of aluminum micro and nanoparticles is presented. The modeling of the oxidation is based on modified Cabrera - Mott model. Heat and mass transfer, both at individual particle level are implemented. The experimental methodology makes use of Thermo-Gravimetry measurements. An investigation of the final oxide layer in the passivation process is carried out for micron and nanometer sized particles. Parametric analysis on the influence of temperature and partial pressure of oxygen are performed. Results are used to estimate and devise a strategy for efficient and safe passivation of aluminum nanopowders.

1. Introduction

Nanoparticle research is currently an area of intense scientific interest due to a wide variety of potential applications in biomedical, optical and electronic fields. They do exhibit size-related properties that differ significantly from those observed in fine particles or bulk materials. Amongst their size-related properties the main one is the extremely high specific area-to-volume ratio. Coupled with aluminum high reactivity makes aluminum nanoparticles a natural choice as solid propellants and nanocomposite energetic materials. While the aluminum powders are highly demanded, the potential to cause undesired explosions when they come in contact with air is clearly a concern. A way to prevent it is to avoid the interaction between the particles and the surrounding environment. The process through which a particle becomes *passive* is called *Passivation*. It consists of covering pure nano-aluminum powders with a thin inactive layer. Amongst different passivation methods, oxidation, a spontaneous and natural phenomena for some metals when exposed to air, is straightforward. In particular some nano metal particles react so fast that explosions can occur. Therefore, the process has to be carried out in a controlled manner, providing a predefined thickness of the oxide film. Analytical and experimental methods are used to investigate the aluminum nanoparticle passivation process.

2. Model formulation

The model describes the formation of a spherical oxide shell according to the Mott - Cabrera mechanism [1]. It is made of two coupled parts. The first describes the oxide layer evolution undergoing isothermal process and the other is controlling the energy involved in the process. The model considers one single nano particle with a conventional metal core and a metal oxide shell (Langmuir layer) that grows once the metal starts to react. The oxidizing environment is made of argon and oxygen. Few assumptions summarized below help to simplify the problem.

- One single nano particle
- Spherical shaped
- Metal internal core of Al
- Low temperature range
- Pre - existing Langmuir layer
- Unchanging volume of the particle

Once the Langmuir layer is formed, the metal electrons starts to escape from inner metal crossing the thin oxide film via tunnel effect. They reach the free side of the passivated layer and ionize the absorbed atoms of oxygen. This mechanism creates an electrostatic potential named *Mott - Potential* between the oxidizer - oxide and the oxide - metal interfaces. The resulting electric field promotes the diffusion of metal cations through the oxide shell. It is always directed from the metal to the oxidizer, so that the direction of the field is outward. It decreases the energy barrier that ions have to jump by a factor of $q\,a|E|$ where q is the charge per unit area at the oxide-oxidizer interface, a is the distance between the energy barrier maximum and the adjacent minimum, while $|E|$ is the absolute value of the electric field that can be evaluated as:

$$E = -\frac{\phi_M}{\delta} \tag{1}$$

where ϕ_M represents the Mott - Potential established within the oxide film and δ is its thickness. As soon as new oxide is formed, the metal core is shrinking. The speed at which it changes can be determine by the equation 2

$$\frac{dV_c}{dt} = A_c\frac{dr_c}{dt} = \Omega I \tag{2}$$

considering V_c the aluminum volume, t the time, A_c is the area of the metal core and r_c its radius, Ω the volume vacated per ion displaced and I the total ions flowing through the oxide layer per second. The ions flow can be estimated:

$$I = A_c n v exp\left(\frac{-U}{kT_p}\right) exp\left(\frac{qa|E|}{kT_p}\right) \tag{3}$$

where n is the number of ions per unit area in the position to jump over the rate limiting energy barrier U, v is the ionic attempt frequency of the jump, k is the Boltzmann constant and T_p is the temperature of the particle. Rearranging, the core radius shrinks as:

$$\frac{dr_c}{dt} = \Omega n v exp\left(\frac{-U}{kT_p}\right) exp\left(\frac{qa|E|}{kT_p}\right) \tag{4}$$

and by a pure subtraction from the initial size of the radius particle r_p, the oxide film is growing according to:

$$\delta(t) = r_p - r_c(t) \tag{5}$$

3. Heat transfer

The oxidation of a pure metal nano particle is a complex process. It involves different physical phenomena that have to be taken into account for realistic modeling. Chemical reaction coupled with the transport of cations, anions as well as electrons, through the oxide layer leads to an oxidation model that should include surface chemistry as well as electrochemistry. In order to take into account all these mechanisms and to reproduce properly the growth of the oxide film, a heat balance is required. Considering m_p the mass of the particle and c_p, T_p respectively its specific heat and its temperature, the heat balance is:

$$m_p c_p \frac{dT_p}{dt} = \dot{Q}_{chem} - \dot{Q}_{rad} - \dot{Q}_{conv} \tag{6}$$

$\dot{Q}_{chem}$ is the chemical heat produced by the Al - O2 reaction, $\dot{Q}_{conv}$ and $\dot{Q}_{rad}$ are the convective and radiative losses. To be more accurate, it would be better to consider the mass of the particle made of aluminum and alumina

$$m_p c_p = m_{Al} c_{Al} + m_{Al2O3} c_{Al2O3} \tag{7}$$

with obvious meaning of each term. The particle is assumed to have the same temperature everywhere due to the small Biot number. The rest of the section is dedicated to the detailed description of the various terms in the energy balance.

3.1 Chemical heat

The chemical heat released is proportional to the grow rate of the oxide shell multiplied by the oxidation enthalpy. It can be expressed as;

$$\dot{Q}_{chem} = 4\pi r_c^2 \frac{dr_c}{dt} \Delta h_{ox} \tag{8}$$

where Δh_{ox} is the enthalpy released from the particle per each mole of Al_2O_3 formed. For atmospheric pressure the diffusion of the gas phase through the particle is not a rate limiting step, but as it will be shown later, for lower partial pressure of oxygen this is not the case. A very small number of O_2 molecules is required to let grow very thin oxide layers. In most cases, the oxygen required is available from a gas layer mean free path lengths of gas molecules. In other words, the predicted reaction will be completed before concentration gradients around the particles are established [2]. Amongst the three heat terms, the chemical power is significant in the first part of the process. As soon as the reaction is slowed down, the other two terms dominate the balance.

3.2 Convective heat

In order to estimate the convective heat, it is firstly necessary to investigate the Knudsen number. It is dimensionless and it is defined as:

$$Kn = \frac{\lambda}{D_p} \tag{9}$$

where λ is the mean free path in the gas and D_p is the particle's diameter. Knudsen number is useful for determining whether continuum or statistical mechanics formulation for fluid dynamics has to be used. If the Knudsen number is near or greater than one, the mean free path of a molecule is comparable to a length scale of the problem and the continuum assumption of fluid mechanics is no longer a good approximation. To estimate the Knudsen number, it is needed to calculate the mean free path of the gas occupying the surroundings. Since oxygen is a diatomic gas, it can be determined by [3]

$$\lambda = \frac{k_t}{P_{O2}} \left[\frac{\gamma - 1}{9\gamma - 5} \right] \sqrt{\frac{8\pi m_{O2} T_\delta}{k}} \tag{10}$$

with k_t the O_2 thermal conductivity, P_{O2} the partial pressure of the gas, γ the specific heat ratio, m_{O2} the mass of the gas molecule, k the Boltzmann constant and T_δ is the temperature at the boundary of the particle considered as the average between the temperature of the particle and the environment. Computing the ratio between λ and D_p the Kn results to be 1.3 for a room temperature. Referring to [3] for nanoparticles of about $100nm$ its value is within the range $0.01 < Kn < 10$, therefore it is in the transition regime. It is now possible to calculate the convective heat, making use of the equation proposed by Fuchs [4] as

$$\dot{Q}_{conv} = \alpha \pi D_p^2 P_{O2} \sqrt{\frac{k T_\delta}{8\pi m_{O2}}} \frac{\gamma + 1}{\gamma - 1} \left(\frac{T_p}{T_\delta} - 1 \right) \tag{11}$$

in which α is the accommodation coefficient and the other terms have the same meaning as before. As soon as the heat is produce by the chemical source the convection heat removes it from the particle.

3.3 Radiative losses

The last term is following the Stefan-Boltzmann's law, transferring heat from the particle to the surrounding. The radiative term is:

$$\dot{Q}_{rad} = \epsilon \sigma A_p (T_p^4 - T_e^4) \tag{12}$$

where ϵ is the emissivity of the particle surface, σ the Stefan-Boltzmann constant, A_p and T_p the area and the temperature of the particle and T_e the environmental temperature. The radiative term is the smallest. It reaches its peak immediately after the chemical production, but as soon as the reaction slows down and that the difference between the two temperature becomes smaller, it's contribution is almost negligible.

4. Experimental procedure

Experiments are performed by a Thermo - Gravimetric Analyser (TGA). It is used to monitor the difference in mass of the nano aluminium sample during the oxidation process and in general during any chemical changes in the powder involving mass changes. From these measurements it is possible to retrieved the history of the oxide layer growth. It is located inside a glovebox with a controlled atmosphere. Parametric analysis is performed to select the experimental conditions that optimize the oxide layer growth.
In order to retrieve the size of the oxide layer from the mass uptakes during oxidation, the fractional changes in mass $\Delta m/m_0$ can be expressed as:

$$\frac{\Delta m}{m_0} = \frac{(z_0 - z_f)}{(1 + z_0)[Q(1 + z_f) + z_f]} \tag{13}$$

where m_0 is the initial sample mass, Q equals 2/3 of the ratio of aluminum to oxygen molecular weights[1] and z_0 and z_f are mass ratios before and after the oxidation. By computing the ratio of the total mass of pure Al to the total mass of alumina in any given sample of Al powder (z), it can be shown the relation between the mass uptake and the atomic fraction of oxygen in the sample $at.\%O$ as:

$$z = \frac{[(300/at.\%O) - 5]}{\beta} \tag{14}$$

where $\beta = 3.78$ is the ratio of alumina to aluminum molecular weights and $at.\%O$ is determined by the equation

$$at.\%O = \frac{300}{[5 + \gamma\beta(x^3 - 1)^{-1}]} \cdot \% \tag{15}$$

with $\gamma = 0.68$ the ratio of Al to alumina densities, x the ratio between is the particle radius r_p and the radius of the Al core r_c and it can be also expressed in function of the thickness of the oxide layer δ as:

$$x = 1 + \delta/r_c \tag{16}$$

5. Results and discussions

5.1 Numerical results

The numerical model consists of a system of two differential equations that have been solved by means of Rounge-Kutta Felbergh method where integration is done with 4th order and accuracy is checked with second order.

$$\begin{cases} \dfrac{dr_c}{dt} = \Omega n v exp\left(\dfrac{-U}{kT_p}\right) exp\left(\dfrac{qa|E|}{kT_p}\right) \\ m_p c_p \dfrac{dT_p}{dt} = \dot{Q}_{chem} - \dot{Q}_{rad} - \dot{Q}_{conv} \end{cases}$$

5.2 Size effect

Different analysis have been performed to predict the final oxide thickness. At room temperature with very low partial pressure, tests were run for five different initial particle's radii : $2.5nm$, $5nm$, $10nm$, $30nm$ and $100nm$. Figure 1 shows the results on a overall time of $2000sec$. The trend is the same for all the curves. There are two growth regimes. The first within $200sec$ in which a fast oxidation rate is present and the smallest particle reaches almost 8Å. The second much slower is appearing as a plateau. A very reduced growth rate of less than 1Å is occurring in the last $1700sec$. This is due to the fact that the freshly formed alumina is obstructing the flow of ions, therefore electrons need more time to reach the aluminum core and to react with it. In addition the curves differ one from each other for their initial sizes. The smallest particle is assumed to have an initial radius of $2.5nm$ while the biggest is of $100nm$. The size effect has to be taken into account. Smaller particles are reacting faster because of their specific area to volume ratio. The different atoms distribution on the surface, makes them freer to move on the surface and to create easily new bounding. Increasing the initial diameter, the size effect is reduced.

---

[1] From the stoichiometric reaction $2Al\ \frac{3}{2}O_2 \rightarrow Al_2O_3$

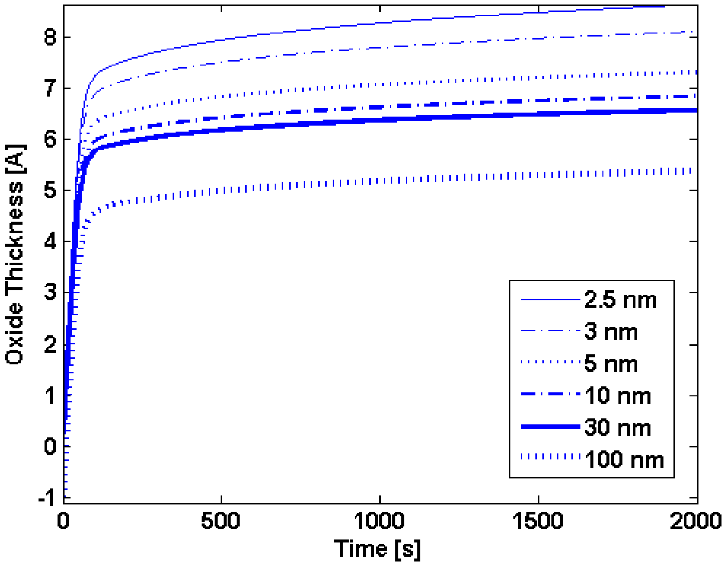

Figure 1: Numerical model of oxide layer thickness versus time for different particle's radii

Considering the temperature of the particle, the fastest is the reaction the hottest is the particle. The heat losses are not able to release all the energy produced during the initial reaction and therefore the particle increases its temperature. This effect specially for very small particles can lead to a dangerous mechanism in which the runaway temperature occurs. Small particles are pyrophoric, e.g. ignite without appreciable initial preheating. Figure 2 shows that smaller is the particle higher and shifted to the right is the temperature peak reached. As the time scale reports, this phenomena is recorded in the very first instants of the passivation process. This is in agreement with the slope of the initial grow rate in Figure 1

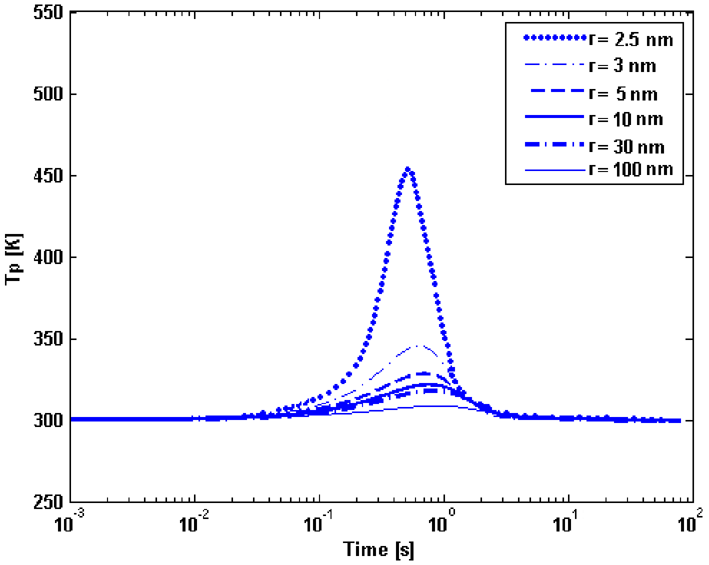

Figure 2: Numerical model of temperature versus time for different particle's radii

5.2.1 Temperature effect

The second test was ran to see how much the environmental temperature is affecting the growth rate of the oxide. Experimental results from Jeurgens [5] were used to validate the model. He demonstrated experimentally that the passivating layer evolution can be split in two different regimes. An initial very fast film growth, and a second much slower oxidation stage which is mostly observed at high temperature. Figure 3 compares the experimental results on a flat cleaned aluminum surface with the ones carried out with the present numerical model. The figure plots with continuous lines the experimental results [5] and with dotted lines the numerical simulations. Five environmental temperature are investigated in the range from 100^oC to 500^oC with low partial pressure of oxygen. The matching with the model at relatively low temperatures is almost perfect. The dynamic and the final thickness reached are well reproducing the experiments. As soon as the temperature increases the model has difficulties to follow the continued curves. The reasons for the mismatch can be multiple. First of all the experiments were performed on a flat metal aluminum surface while the model reproduces the test for one single aluminum particle of $100nm$. The size effect is present but since the particle is big enough the model neglects it. What is neglected in the numerical model is the interaction between particles that becomes significant at high temperatures. In addition at higher temperatures the Cabrera - Mott mechanism is replaced by the diffusion through the porous media specially in the case of flat plate.

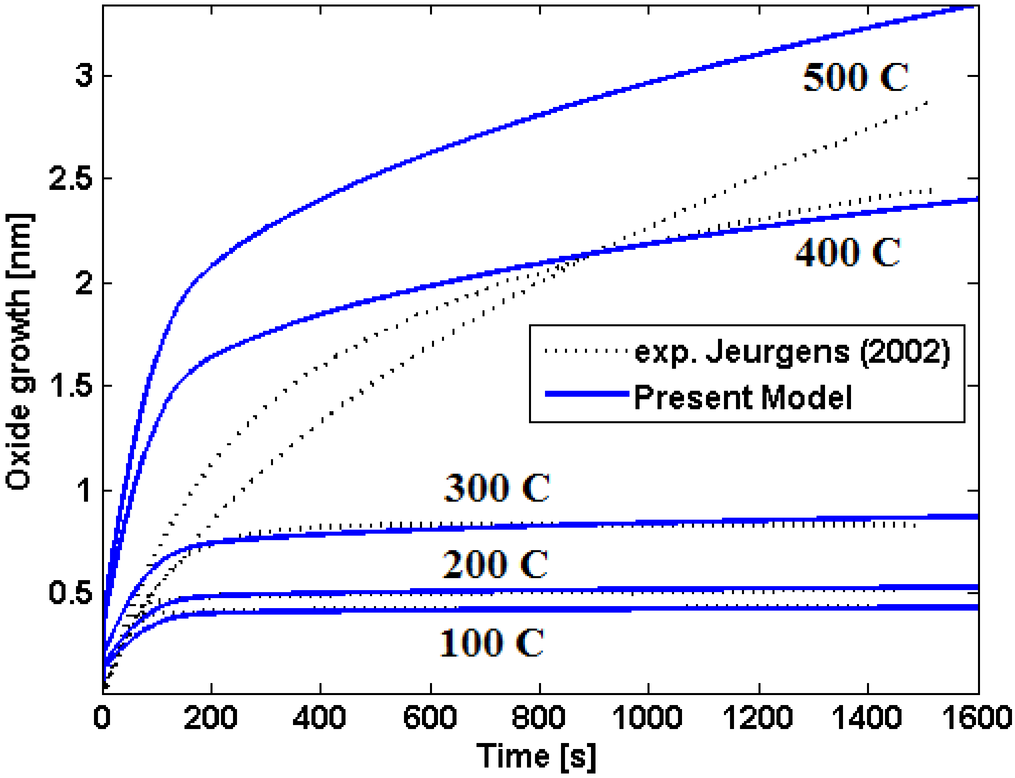

Figure 3: Experimental [5] and numerical evolutions of the oxide growth at different temperatures, P_{O2} equals $1e^{-4}$ Pa

5.2.2 Partial pressure of oxygen effect

The same type of investigation has been carried out analyzing the influence of partial pressure of oxygen on the final oxide layer. Experiments performed by Cai [2] with a flat cleaned aluminum surface were used as references to compare the numerical results. Four different oxygen partial pressure are studied: $1e^{-6}Pa$, $1e^{-5}Pa$, $1e^{-4}Pa$ and $1e^{-3}Pa$ at room temperature. Above this pressure no relevant changes are detected. The continuous curves result from the present numerical model while the dotted curves are experimental. The dynamic of the curves is respected. The final thickness is predicted with a small constant error that is in the range of a couple of Å. It can be concluded that the higher is the concentrations of oxygen the more significant is the increase of the thickness of the final oxide layer. On the contrary smaller values of P_{O2} are not able to provide enough oxygen to the aluminum surface and therefore the growth is slowed down.

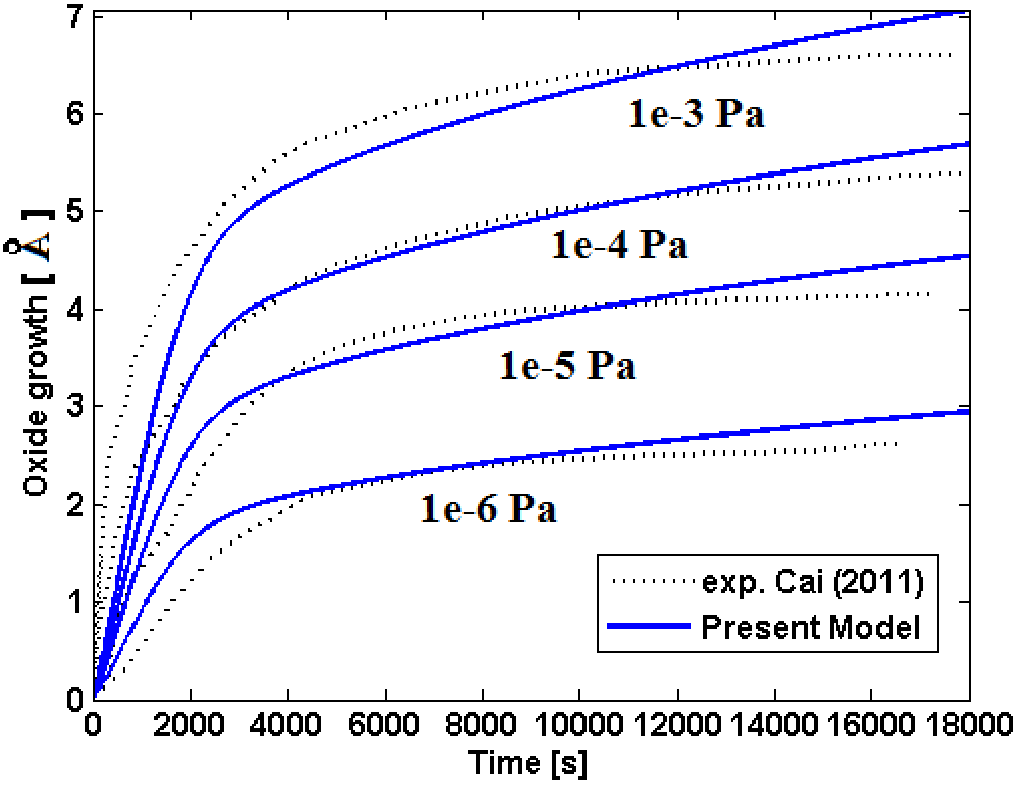

Figure 4: Experimental [2] and numerical evolutions of the oxide growth at different P_{O2}, T equals $300K$

5.3 Experimental results

The first part of the experimental testing investigates the different reactivities of micro and nano powders of aluminum undergoing the passivation process. A parametric analysis was than performed on nanoparticles to study the influence of temperature in terms of speed of reaction and thickness of the oxide layer. All the tests are carried out using aluminum powders with a mean diameter of 120nm with argon as protective gas and oxygen as oxidizer.

5.3.1 Aluminum micro versus nano particles

A comparison between micro and a nano sample of aluminum is here presented. The purpose is to underline how different is the passivation process in the two cases. Table 1 shows the experimental conditions used.

Test settings	**Value**
O2 concentration	20 %
O2 flow	70 ml/min
Ar flow	20ml/min
Heating Rate	20 K/min
Temperature ramp	30^oC to 1200^oC

Table 1: Experimental conditions for dynamic tests with micro and nano powders

Figure 5 a), plots the comparison of the TGA analysis. Dotted curve is the nanopowder signal, while the continuous line is for micropowder. The results show that by the end of the test the mass increase in the nanopowder sample is five times bigger than the one of micropowders. The size effect of the aluminum powders is so important that even the effect of a pre-existing passivation layer becomes negligible in respect to that. Indeed, the initial passivated layer of the two samples was different. Microparticles had a mean diameter of 50μm and they were unpassivated. On the contrary nanoparticles were covered with a film of polymers over a coat of alumina. For this reason the first part of the test with nanoparticles detects a mass decrease due to the evaporation of the polymer layer. After that, the different expansion coefficients of alumina and aluminum due to temperature increases causes cracks. Therefore the oxidation level is enhanced. On the other hand, since no layers were present in the micron sized sample, no mass reductions and no cracks occurred. At the end of the temperature program, the nano sample finished its oxidation process, while the microparticles just started. In order to see how much more time the second sample needed to reach a higher oxidation level, the test for micro was continuing longer. Because of the furnace limits, it was not possible and safe to increase more the temperature. Therefore an isothermal program at 1200^oC was set and kept for almost one week. The results are showed in Figure 5 b) and listed in Table 2.

Sample	δ_f**[nm]**	**oxidation time**
nano	17.66 nm	60 min
micro	9.63 μm 168 h	

Table 2: Final thickness and oxidation time after the dynamic tests with micro and nano powders

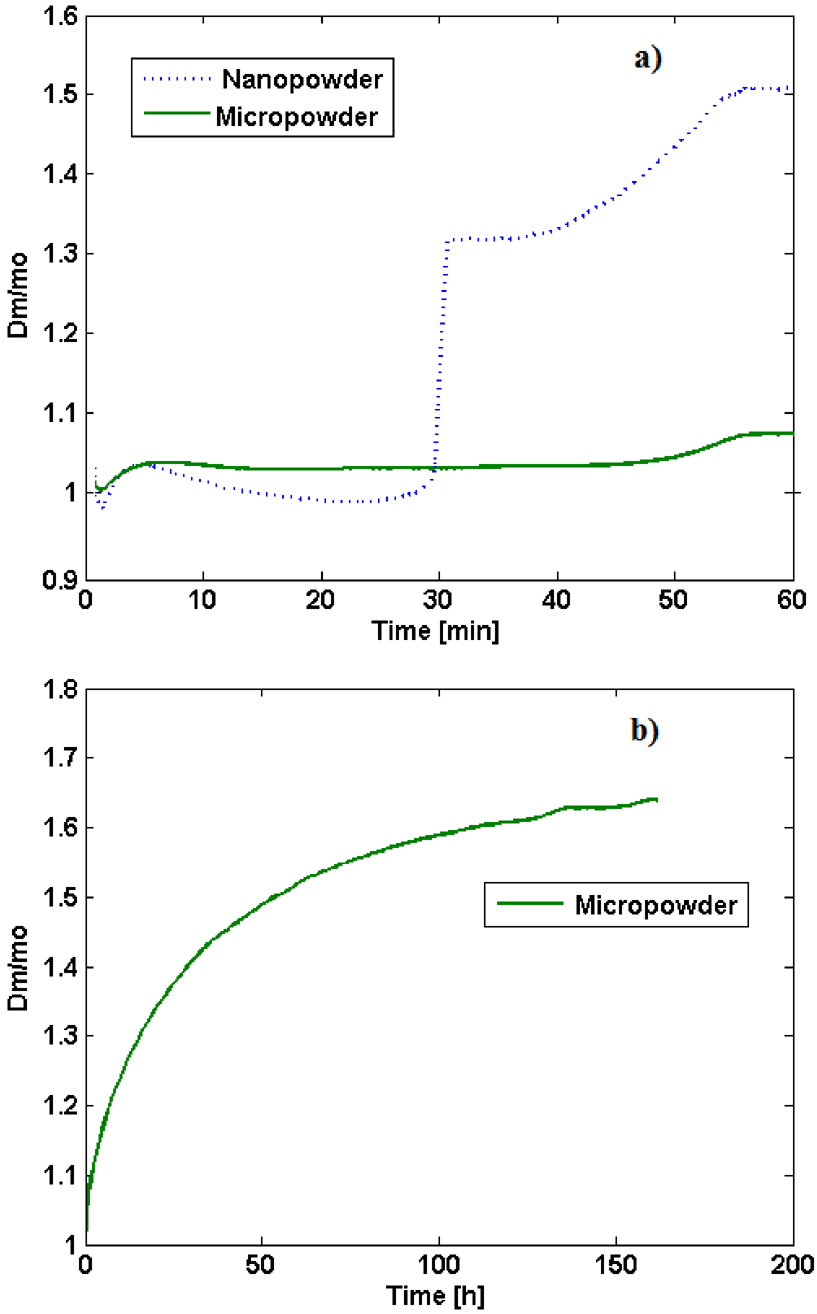

Figure 5: TGA measurements. a) Mass uptake evolutions for the dynamic tests with micro and nano powders. b) Mass uptake evolution after one week of isotherma program at 1200^oC with micro powder

Figure 6 shows the two samples of micro and nano sizes. They underwent the same dynamic temperature program described in Table 1. The main difference is in the color of the samples. The nanopowder changed it from gray to fully white. The aluminum is transformed into oxide and it still looks like a powder. On the contrary the sample with microparticles is grayer and is a mono piece of metal stacked at the bottom of the crucible that is no more reusable.

Figure 6: Image of the samples after the dynamic test. Micro and nano particles respectively on the left and on the right side

5.3.2 Aluminum nanoparticles : temperature effect

Three isothermal temperatures were used: 400^oC, 500^oC and 600^oC. Fixed heating rate of $20K/min$ to reach the different isothermal levels, fixed mass flow rate and fixed oxygen concentration are reported in Table 3.

Test settings	**Value**
O2 concentration	20 %
O2 flow	50 ml/min
Ar flow	$20ml/min$
Heating Rate	20 K/min
Isothermal Temperature	variable

Table 3: Isothermal temperature programs for the parametric analysis on temperature with nanopaticles

Figure 7 plots the δ evolution only during the isothermal part of the measurements. The three curves are shifted to a common starting point that corresponds to the end of the evaporation of the polymer layer. Isothermal temperatures are maintained for $2h$. The sample at 400^oC does not measures any further oxidation due to the pre-existing passivated alumina layer and the low temperature. The test at 500^oC detects a constant increase of the film thickness. After two hours of test, the oxide reaches almost $6nm$. For the test at 600^oC an immediate and brutal oxidation occurs providing in the first minutes a δ growth of about $4nm$. After this very fast rate, the curve reduces its slope. The sharp step at 600^oC is caused by the presence of cracks in the oxide layer. They allow the aluminum to come in contact with oxygen much faster. Table 4 synthesized the final parameters.

Tempreature	δ_f**[nm]**	**oxidation level [%]**
400^oC	2.06 nm	0.1
500^oC	5.25 nm	9.33
600^oC	7.99 nm	19

Table 4: Final thickness and oxidation level after the parametric analysis on temperature with nanoparticles

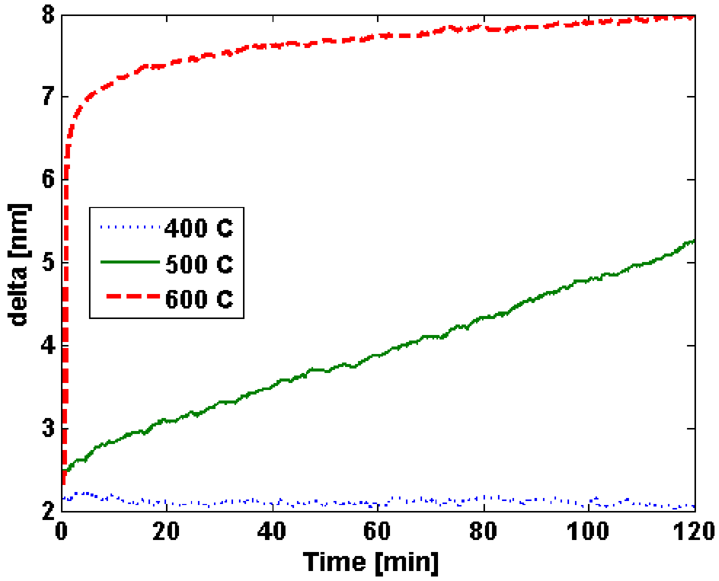

Figure 7: Experimental evolution of the oxide growth at different temperatures with nanoparticles

5.3.3 Numerical model and experimental results: comparison

The last part of this section is dedicated to the validation of the numerical model with the present experimental tests. By initializing numerically the pre-existing alumina layer of the nanopowder to 1.9 *nm*, it was possible to retrieve the effect of temperature on the final oxide thickness.

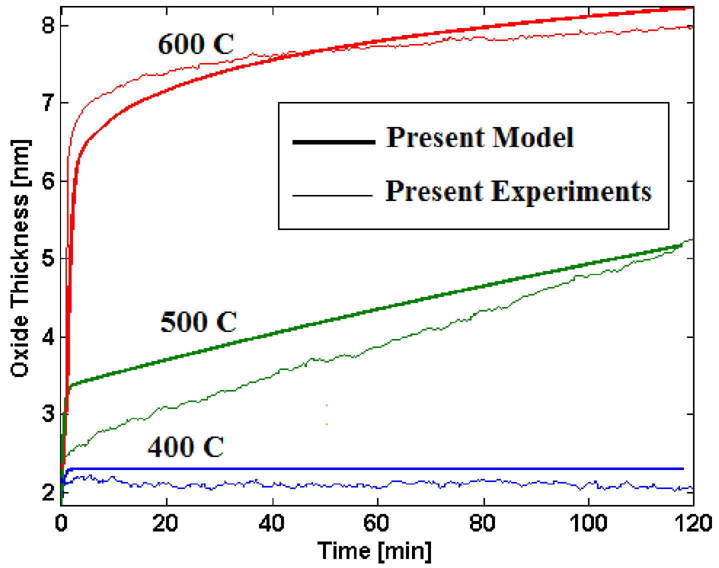

Figure 8: Experimental and numerical evolution of the oxide growth at different temperatures with nanoparticles

Figure 8 plots thinner the experimental results and thicker the numerical ones. The isothermal tests reported are the same as before. The fitting at the relatively low temperature of 400^oC is satisfactory, as well as for the highest temperature of 600^oC. Mismatching is visible for the test at 500^oC. In the initial part the two curves predict layers of almost 1 *nm* different. The discrepancy is reduced by time and can be due a limit of the model.

6. Conclusions and future works

The industrial prototype of aluminum nanoparticles production includes a passivation unit where particles undergo the oxidation process. Numerical and experimental methods have been successfully used to estimate and devise a strategy for efficient and safe passivation of aluminum nanopowders. The variables that identify a satisfactory passivation level are the thickness of the oxide layer and the its oxidation time.

The extended version of the numerical Mott - Cabrera model well suits the oxidation mechanism for aluminum nanopowders. Temperature ranges below the aluminum melting point of 660^oC and small oxide thickness to guarantee the crossing of ions via tunnel effect represent the physical limits for this model, thus it is adequate to estimate passivation in the context of the present project. The differential equations allow to solve the electrochemical phenomena and to record its thermal history. They predict the growth of the oxide layer by taking into account the particle sizes and their temperatures. The model estimates that at room temperature and low partial pressure a particle of $2.5nm$ radius leads in about 30 min to films in the range of $1nm$ with an increase of temperature of $150[K]$. The numerical simulation is capable to well reproduce the influence of various environmental temperatures and partial pressures of oxygen. The model is validated with experimental results found in literature.

Dynamic tests with a heating rate of 20 K/min were used to compare micron and nanometer sized particles. Under the same experimental conditions with a final temperature of 1200^oC the nano sized sample reached an oxidation level of almost 60% after only 1 h. In the same time the oxidation level reached by the sample with micro sized particles was less than 10 $\%$. It was necessary to keep the sample at 1200^oC for other 140 h to obtain approximately the same level (see Figure 5).

The influence of temperature on the final thickness layer is investigated with isothermal programs. Tests at 400^oC, 500^oC and 600^oC showed three totally different behaviors. At 400^oC almost no growth was detected due to the alumina coat of the sample that did not allow any further oxidation. At 500^oC the alumina layer grown linearly to $5.25nm$. For the test at 600^oC a sharp increase of 15 $\%$ in the TG measurements within few seconds occurs. After that the growth is practically over.

Future works would include an extension of the numerical model to a multi - particle approach that could help to solve the small discrepancies with the literature. A direct comparison with the experimental results was not satisfactory for the present work due to the very poor characterization of the samples used. All the investigated nano particles were provided of coat of alumina and than polymer layer. In further work, it would be of utmost importance to test unpassivated nanoparticles. This could be very helpful because it would represent the direct link between the model, the literature and the experiments in terms of size and coating layer. Therefore the very first suggestion to pursue this work could be the use of nanoparticles without any alumina or polymer passivation layer. In alternative nanosized particle covered with polymers could also be a good choice. Knowing the evaporation of the polymers and their products of reaction, it could be possible to remove them and to start after the oxidation study.

Acknowledgments

The financial support of this work is provided by the Wallon Region under the convention 6405 which is gratefully acknowledged. A thanks to Gertjan Glabeke for his technical contribution in the labs.

References

[1] N Cabrera and N F Mot. 1949. Theory of the oxidation of metals. In: *Reports on Progress in Physics*.

[2] Cai, Na and Zhou, Guangwen and Muller, Kathrin and Starr, David E. 2011. Tuning the Limiting Thickness of a Thin Oxide Layer on Al(111) with Oxygen Gas Pressure. In: *Phys. Rev. Lett.*.

[3] Mohan, Salil, Trunov, Mikhaylo A., Dreizin, Edward L. 2012. Heating and Ignition of Metal Particles in the Transition Heat Transfer Regime. In: *Journal Heat Transfer*.

[4] Fuchs N. A. 1963. On the Stationary Charge Distribution on Aerosol Particles in a Bipolar Ionic Atmosphere. In: *Geofis. Pura Appl.*.

[5] L. P. H. Jeurgens and W. G. Sloof and F. D. Tichelaar and E. J. Mittemeijer. 2002. Growth kinetics and mechanisms of aluminum-oxide films formed by thermal oxidation of aluminum. In: *Journal of Applied Physics*.

[6] Juan Sun and Michelle L. Pantoya and Sindee L. Simon. 2006. Dependence of size and size distribution on reactivity of aluminum nanoparticles in reactions with oxygen and MoO3. In: *Thermochimica Acta*.

[7] Park, K. and Lee, D. and Rai, A. and Mukherjee, D. and Zachariah, M. R. 2005. Size-Resolved Kinetic Measurements of Aluminum Nanoparticle Oxidation with Single Particle Mass Spectrometry. In: *The Journal of Physical Chemistry B*.

[8] Stephen W. Chung and Elena A. Guliants and Christopher E. Bunker and Paul A. Jelliss and Steven W. Buckner. 2011. Size-dependent nanoparticle reaction enthalpy: Oxidation of aluminum nanoparticles. In: *Journal of Physics and Chemistry of Solids*.

[9] Tran X. Phuoc and Ruey-Hung Chen. 2012. Modeling the effect of particle size on the activation energy and ignition temperature of metallic nanoparticles. In: *Combustion and Flame*.

[10] Trunov, Mikhaylo A. and Umbrajkar, Swati M. and Schoenitz, Mirko and Mang, Joseph T. and Dreizin, Edward L. 2006. Oxidation and Melting of Aluminum Nanopowders. In: *The Journal of Physical Chemistry B*.

[11] Yun, Gi-Sang and Kwon, Young-Soon and Kim, Ji-Soon and Kim, Jin-Chun and Ilyin, AlexanderP. 2010. Excess energy in the electroexplosive nanopowders. In: *Research on Chemical Intermediates*.

[12] R. Nakamura and D. Tokozakura and H. Nakajima and J.-G. Lee and H. Mori. 2007. Hollow oxide formation by oxidation of Al and Cu nanoparticles. In: *Journal of Applied Physics*.

[13] Richard Ghez. 1973. On the Mott-Cabrera oxidation rate equation and the inverse-logarithmic law. In: *The Journal of Chemical Physics*.

[14] Alexandre Ermoline and Edward L. Dreizin. 2011. Equations for the Cabrera-Mott kinetics of oxidation for spherical nanoparticles. In: *Chemical Physics Letters*.

[15] Aumann, C. E. and Skofronick, G. L. and Martin, J. A. 1995. Oxidation behavior of aluminum nanopowders. In: *Journal of Vacuum Science Technology B: Microelectronics and Nanometer Structures*.

[16] Mohan, Salil and Ermoline, Alexandre and Dreizin, EdwardL. 2012. Pyrophoricity of nano-sized aluminum particles. In: *Journal of Nanoparticle Research*.

[17] Cai, Na and Zhou, Guangwen and Muller, Kathrin and Starr, David E. 2012. Temperature and pressure dependent Mott potentials and their influence on self-limiting oxide film growth. In: *Applied Physics Letters*.